# Effects of strain rate in laser forming

Wenchuan Li and Y. Lawrence Yao
Department of Mechanical Engineering, Columbia University
New York, New York 10027, USA

## Abstract

Experimental investigation and numerical simulation of the influence of the strain rate in laser forming are presented. To isolate and effectively study the strain rate effects, which are temperature dependent, a "constant peak temperature" method is developed with the aid of numerical modeling and solution. Under the condition of the constant peak temperature, the effects of strain rate on forming efficiency, residual stress and hardness of the formed parts are studied both experimentally and numerically. In the numerical model, the temperature dependence and strain-rate dependence of the flow stress and other material properties are considered. The simulation results are consistent with the experimental observations. The micro-structural changes of the formed parts are also presented.

## 1. Introduction

Laser forming is a process in which laser-induced thermal distortion is used to form sheet metal without a hard forming tool or external forces. It is therefore a flexible forming technique suitable for low-volume production and/or rapid prototyping of sheet metal, as well as for adjusting and aligning sheet metal components[1]. Aerospace, shipbuilding, microelectronics and automotive industries have shown interest. A simple type of the laser forming is straight-line laser bending (Fig.1) and forming more involved shapes has been shown possible.

Understanding various aspects of the laser forming is a challenging problem of considerable theoretical and practical interest. Experimental and theoretical investigations have been reported to understand the mechanisms involved in the laser forming. The proposed mechanisms are temperature gradient mechanism (TGM)[2], buckling mechanism (BM)[3], and upsetting mechanism depending on operation conditions, material properties and workpiece thickness. A number of analytical models were derived to predict the bending angle $\alpha_b$ (Fig.1) in the straight-line laser bending[2]. Some of the models are in reasonable agreement with experimental results. More detailed studies were conducted via numerical investigations. Vollertsen, et al.[4], Hsiao, et al.[5], and Alberti, et al.[6] simulated the process using the finite element or finite difference method. In these numerical studies, the bending angle was computed and compared reasonably with experimental results. Additional information, such as temperature, stress and strain distribution and time history were also extracted for more detailed analysis. Parametric studies of process parameters, workpiece geometry and material properties on the laser forming process were reported, such as influence of strain hardening, and edge effects[7, 8]. Issues of working accuracy, and aerospace alloy application have also been reported.

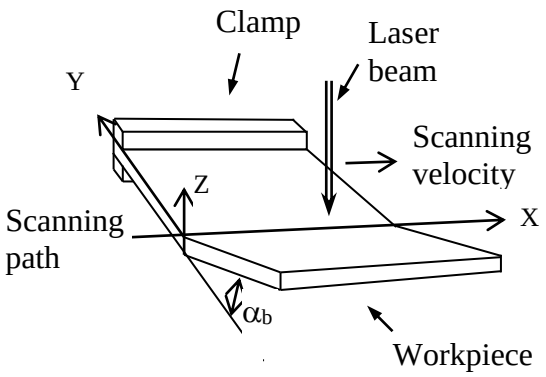


Fig. 1 Schematic of straight-line laser forming

The effects of strain rate in the laser forming, however, have not been studied in detail. In the laser forming, the strain rate could reach two per second under commonly used laser power levels and laser scanning velocities. Although this level of strain rate is not high as compared with that experienced in some other metal forming processes, temperature in the laser forming could rise close to the melting point of the workpiece material. As known, the strain rate at elevated temperatures has much higher influence on the material flow stress than at lower temperatures. The influence on the flow stress translates to that on the forming process and properties of the formed parts, including residual stresses and hardness of the formed parts.

Experimental results showed that the bend angle $\alpha_b$ in the straight-line laser bending is directly proportional to $v^{-1/2}$ for low-carbon steel plates[2,], where $v$ is the laser scanning velocity (therefore associated with the strain rate). The main reason that the bend angle decreases with increasing velocity is that the laser energy input per unit time reduces when the scanning velocity increases. The bend angle decrease is also due to flow stress increase because the higher the velocity, the higher the strain rate, which causes the flow stress to rise. Therefore, aforementioned relationships represent the effects of both the input energy and the strain rate on the bending process. One may think that a better approach to explore the strain rate effects is to ensure a constant laser energy input per unit length. To achieve that, one may keep "line energy" constant. The line energy is defined as $P/v$, where $P$ is the laser power. If the units of $P$ and $v$ are W and m/s, the unit of the line energy is J/m. So the line energy represents the energy input per unit length along the scanning path. Under the condition of constant line energy, although the laser energy input per unit length is kept constant, the net energy input available for the forming purpose may still vary due to different heat dissipation rates associated with different scanning velocities[9]. Therefore, investigations under the condition of constant line energy are still not ideal to study the strain rate effects. The ideal scenario is to ensure the net energy input available for the forming purpose constant while varying the strain rate. In this way the strain rate effects can be isolated and studied without interference of other variables.

In this work, strain rate effects in laser bending are studied under the condition of "constant peak temperature," that is, the combinations of laser power and scanning velocity are so determined that the peak temperature reached at the top surface of the laser scanned workpiece remains constant. In this way the constant net energy input available for the forming purpose can be maintained under different scanning velocity (strain rate). A numerical model based on the finite element method is developed to aid the determination of the process parameter values that give the constant peak temperature. The same model is also used to predict the effects of strain rate on bending angle and residual stress among others. The numerical results are experimentally validated.

## 2. Strain rate and effects

For a given temperature, the strain rate in terms of tensor $\dot{\underline{\underline{\varepsilon}}}$ can be written as

$$\dot{\underline{\underline{\varepsilon}}} = \frac{1}{2}\left(\frac{\partial \underline{v}}{\partial \underline{x}} + \left(\frac{\partial \underline{v}}{\partial \underline{x}}\right)^{T}\right) \tag{1}$$

where $\underline{v}$ is the particle velocity vector and is defined as $\underline{v} = \frac{\partial \underline{x}}{\partial t}$ when the Lagrangian viewpoint is taken, $\underline{x}$ is the spatial position vector of a material particle at time $t$, and $\frac{\partial \underline{v}}{\partial \underline{x}}$ is the velocity gradient, all in the current configuration.

The stress and strain tensor, $\sigma_{ij}$ and $\varepsilon_{ij}$, can be decomposed into their mean portions and their deviatoric portions, that is, $\sigma = \sigma_{ii}/3$, $\varepsilon = \varepsilon_{ii}/3$, $s_{ij} = \sigma_{ij} - \delta_{ij}\sigma$, and $e_{ij} = \varepsilon_{ij} - \delta_{ij}\varepsilon$, where $\sigma$ and $\varepsilon$ are mean portion, $s_{ij}$ and $e_{ij}$ are deviatoric portions, and $\delta_{ij}$ is the Kronecker delta. For work-hardening materials, the relationship between deviatoric stress and plastic strain rate $\dot{e}_{ij}^{\,pl}$ by taking into consideration of temperature influence can be written in terms of tensor[10].

$$\dot{e}_{ij}^{\,pl} = 0, \qquad \text{if } f < 0, \text{ or if } f = 0 \text{ and } \left(\frac{\partial f}{\partial s_{ij}}\dot{s}_{ij} + \frac{\partial f}{\partial T}\dot{T}\right) < 0$$

$$\dot{e}_{ij}^{\,pl} = -\frac{1}{\dfrac{\partial f}{\partial e_{ij}^{\,pl}}}\left(\frac{\partial f}{\partial s_{kl}}\dot{s}_{kl} + \frac{\partial f}{\partial T}\dot{T}\right), \quad \text{if } f = 0 \text{ and } \left(\frac{\partial f}{\partial s_{ij}}\dot{s}_{ij} + \frac{\partial f}{\partial T}\dot{T}\right) \geq 0 \tag{2}$$

Eq. 2 represents the general relation of stress, strain and their rates, in terms of tensor and with temperature consideration. In practice, however, similar relationships are often empirically determined under the one-dimensional condition and applied to multi-dimensional cases using the concept of equivalent stress and strain. Much effort therefore has been made to determine the flow stress dependence on strain rate and temperature for the one-dimensional case. For a deformation process of metals with a strain rate, $\dot{\varepsilon}$, and temperature, $T$, the stress, $\sigma$, is given by

$$\sigma = C'\dot{\varepsilon}^{m}e^{\frac{mQ}{RT}} = C\dot{\varepsilon}^{m} \tag{3}$$

where $m$ is the strain-rate sensitivity exponent, $Q$ the activation energy , $R$ the gas constant, both coefficient $C$ and $m$ depend on temperature and material.

## 3. Numerical simulation

To simulate the strain rate effects in laser forming, reasonable values of the strain-rate sensitivity exponent $m$ and flow stress at different temperatures were obtained from available literature. Work hardening was also taken into consideration. The simulation of the laser forming process was realized by a thermal-structure analysis using commercial finite element

analysis code ABAQUS. For thermal and structural analysis, the same mesh model is used. In order to simulate the shear process in the laser forming, a three-dimension element with twenty nodes was used because this kind of element has no shear locking and hourglass stiffness and is also compatible with thermal stress analysis. A user-defined FORTRAN program was necessary to model the heat source input from the Gaussian laser beam.

The main assumptions used in the numeral simulation of laser forming are as follows. The materials simulated in this work are isotropic and continuous. Plastic deformation generated heat is small as compared to energy input in the laser forming so that it is negligible. During the entire laser forming process, no melting takes place. The forming process is symmetrical about the laser-scanning path (Fig. 1).

The boundary conditions used include that the top surface is cooled by a weak gas flow. The remaining surfaces are cooled through free convection with atmosphere. Across the symmetric plane (the X-Z plane in Fig. 1), the movement of materials does not occur. The symmetric surface is under the adiabatic condition. Surface heat flux follows $q = q(\underline{x}, t)$, surface convection $q = h\,(T - T^o)$, where $h = h(\underline{x}, t)$ is the film coefficient, and $T^o = T^o(\underline{x}, t)$ the surrounding temperature, and radiation $q = A((T - T^z)^4 - (T^o - T^z)^4)$, where $A$ is the radiation constant and $T^z$ the absolute zero on the temperature scale used.

## 4. Experiment

As discussed early, in order to study the strain rate effects in an isolated manner, it is desirable to create conditions under which strain rate may vary but net energy input available for the forming purpose remains constant. To approximate the scenario, a constant peak temperature method was devised. In determining the process parameters for the condition of constant peak temperature, the scanning velocities are specified first and the laser powers were iteratively determined using the numerical simulation to give approximately the same peak temperature at the top surface of the workpiece. Listed in Table 1 are values determined for a targeted peak temperature of 1,030°C.

Table 1 Experimental and simulation condition under constant peak temperature

| Velocity (mm/s) | 80 | 90 | 100 | 110 | 120 | 140 | 170 |
|---|---|---|---|---|---|---|---|
| Power (W) | 800 | 843 | 886 | 929 | 970 | 1040 | 1130 |

Please note that for a specific combination of velocity and power, the peak temperature remains approximately constant throughout the scanning path except at both ends of the path [8]. This fact makes the constant peak temperature method possible where the peak temperature refers to the peak temperature throughout the path and ignores the temperature change at both ends of the path.

For comparison purpose, experiments were also conducted under the condition of constant line energy. The conditions listed in Table 2 are for 10 J/mm.

Table 2 Experimental and simulation condition under constant line energy

| Velocity (mm/s) | 40 | 60 | 80 | 100 | 120 | 135 | 138 |
|---|---|---|---|---|---|---|---|
| Power (W) | 400 | 600 | 800 | 1000 | 1200 | 1350 | 1380 |

Laser bending experiments were carried out with a PRC1500 $CO_2$ laser system with the maximum power of 1.5 kW. The distribution of the power density is Gaussian ($TEM_{00}$). The diameter of the laser beam used is 4mm, which is defined as the diameter at which the power density becomes $1/e^2$ of the maximum power value. The samples were made of low carbon steel AISI 1010 and 80 mm by 40 mm by 0.89 mm in size, with 40 mm along the scanning direction. The samples were first cleaned using propanol and then coated with graphite coating to obtain relatively known and increased coupling of laser power. The geometry of the samples was measured before and after laser forming using a coordinate measuring machine. During the laser scanning, the samples were clamped at one side (Fig. 1). The bend angle may vary slightly along the scanning direction and an average angle was calculated for each sample after measuring at a few locations along the scanning direction.

The residual stress was measured using X-ray diffractometry. Samples obtained from the bent sheet for microstructure observation were mounted, polished, and etched using 3% $HNO_3$ for 20 seconds. The samples were observed under a scanning electron microscope.

## 5. Results and discussion

The results under the condition of constant line energy are briefly presented first (Figs. 2 and 3) to show that the condition in fact is not ideal for studying the effects of the strain rate. The rest of results are obtained under the condition of constant peak temperature. All results of temperature, strain and stress are for the scanning path, either at the top or bottom surface of the workpiece.

### 5.1 Constant line energy

Fig. 2 shows the variation of bend angle with scanning speed under the constant line energy of 10 J/mm (Table 2). It is seen that at lower velocities, the bend angle is smaller despite the line energy is kept constant. This is because that, when the scanning velocity is lower, through-thickness temperature gradient is smaller. This, in turn, makes the difference between the thermally-induced distortions at the top and bottom surfaces smaller. More importantly, heat dissipation is more significant at lower speeds and that makes the efficiency of the forming process to decrease. The numerical results closely agree with the experimental data.

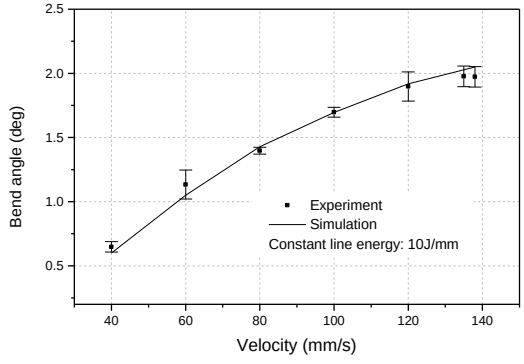


Fig. 2 Comparison under constant line energy (Condition: Table 2)

The above explanation is confirmed by the simulated time history of temperature along the scanning path shown in Fig.3. As seen, the peak

temperature increases with the velocity even when the line energy is kept constant. This is obviously due to less heat dissipation at the higher velocities. In addition, the temperature difference between the top and bottom surfaces increases with velocity for the same reason.

Figs. 2 and 3 show that the condition of constant line energy is not ideal for studying the effect of strain rate. At higher velocities, the strain rate increases and so does the temperature. The increase of strain rate causes increase of flow stress but the increase of temperature causes flow stress to fall. It is therefore difficult to pinpoint the effects of the strain rate. The rest of results are obtained under the condition of constant peak temperature.

## 5.2 Constant peak temperature

As seen from Fig. 4, for the specified velocities, the laser power levels are determined to give approximately the same peak temperature of 1,030$^{o}$C at the top surface of workpiece (Table 1). Although the same peak temperature at the top surface does not necessarily mean the same temperature distribution and thermal process, the method of constant temperature ensures the effect of temperature on flow stress relatively small and allows one to focus on studying the effects of strain rate (scanning velocity).

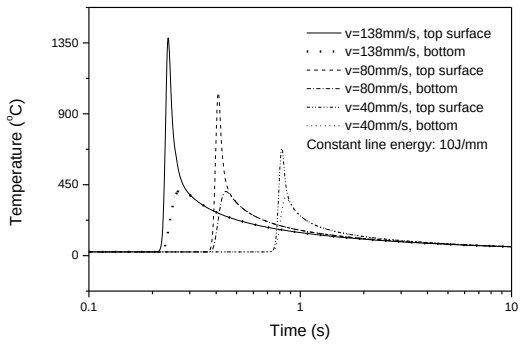


Fig.3 Simulated time histories of temperature under constant line energy

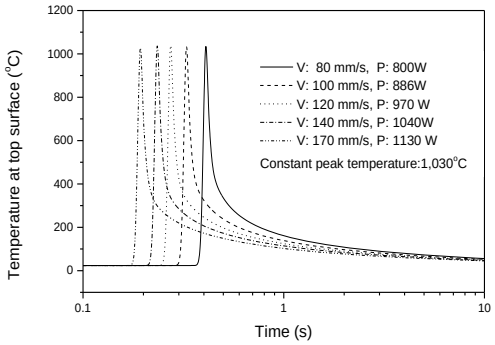


Fig. 4 Simulated time histories of temperature under the condition of constant peak temperature

It is worth to point out that under the condition of constant peak temperature, the laser power still increase with the scanning velocity but does not increase as fast as under the condition of constant line energy. The line energy therefore decreases with increase of the scanning velocity (Fig. 5). This is quite understandable because the more significant heat dissipation at lower velocities requires higher line energy to reach the same peak temperature.

Fig. 6 compares the simulation and experimental results of the bend angle vs. velocity. In Fig. 7, a comparison of numerical simulation and experimental results is made for the Y-axis residual stress on the top surface of the workpiece. The yield stress of the material used at room temperature is about 265 MPa. In both figures, the simulation results agree with experimental measurements. The trends, namely, the bend angle decreasing and residual stress increasing with the increase of scanning velocity (strain rate) are consistent with the understanding of the forming mechanisms. They will be further explained, along with results of strain rate and stress time history.

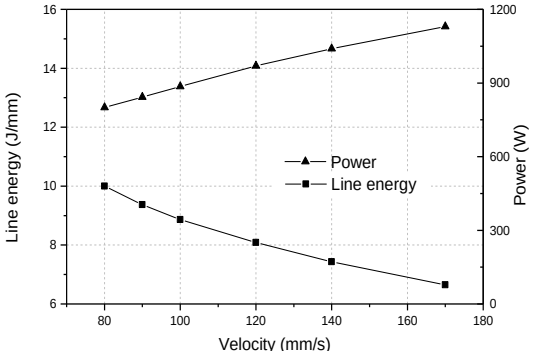


Fig. 5 Line energy and power vs. scanning velocity under the condition of constant peak temperature (Table 1)

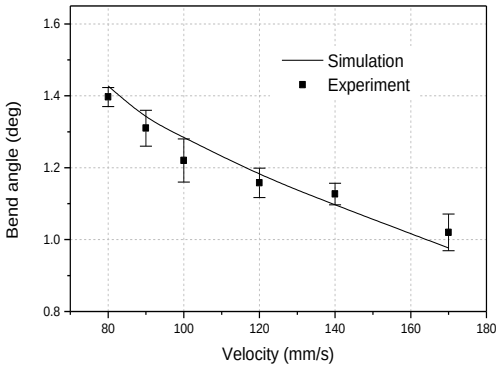


Fig. 6 FEM and experimental results under the condition of constant peak temperature (Table 1)

Fig. 8 presents a typical time history of plastic strains in the Y direction. As seen, the plastic strain is compressive on the upper surface and tensile on the lower surface, which is quite typical for laser forming under the temperature gradient mechanism (TGM). A steep thermal gradient through the thickness leads to a much higher tendency of thermal expansion at the top surface. But surrounding workpiece material restricts the expansion, resulting significant plastic deformation near the top surface. At the cooling stage, the material that has been compressed in the upper layers contracts so that a shortening of these layers make the workpiece bend towards the laser beam, while the lower layers undergo a slight tension (sometime a slight compression resulted from the heating stage remains). Fig. 9 shows that, as the scanning velocity increases, the compressive plastic deformation at top surface becomes smaller. This is obviously due to the increase in strain rate associated with the increased velocity (Fig. 10). The increased strain rate in turn causes the increase in flow stress, which makes bending difficult at the increased velocity. Please note that under the constant peak temperature condition, the results in Fig. 9 primarily represent the effect of strain rate on flow stress because the effect of temperature on flow stress can be neglected. Comparing Figs. 6 and 10, it can be seen that the bend angle decreases about 30% for the nearly doubled strain rate.

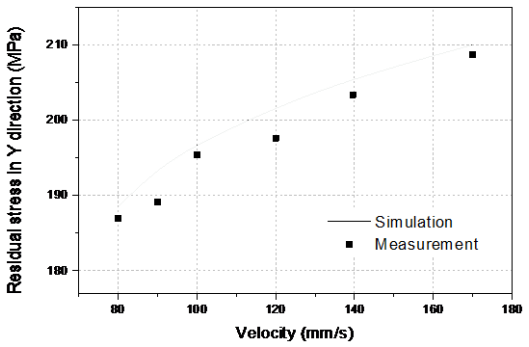


Fig.7 FEM and X-ray diffraction measurement of residual stress under the condition of constant peak temperature (Table 1)

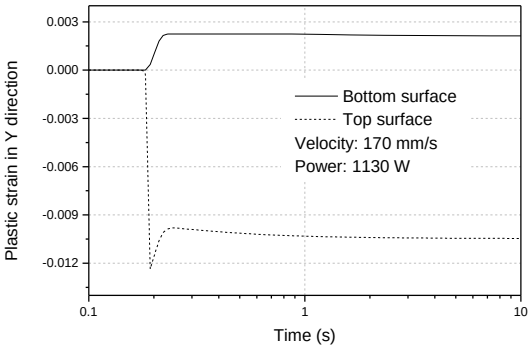


Fig. 8 Typical time histories of plastic strains in the Y direction under the condition of constant peak temperature

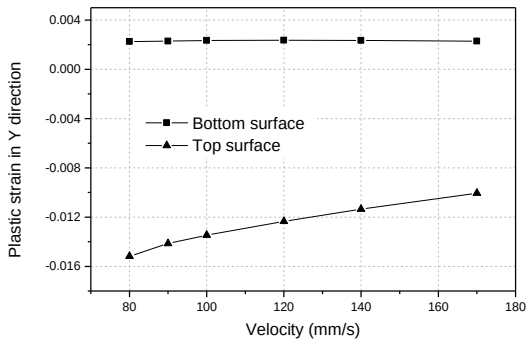


Fig. 9 Plastic strain in Y direction vs. velocity (constant peak temperature)

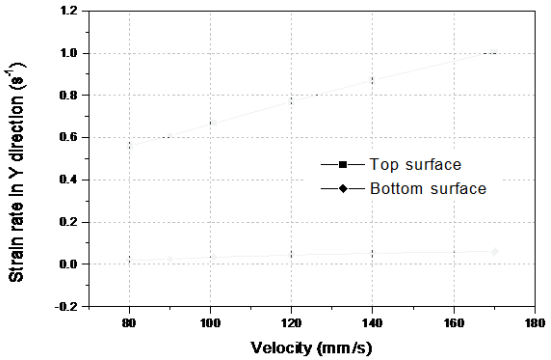


Fig.10 Strain rate in Y direction vs. velocity (constant peak temperature)

## 5.3 Residual stress

To better understand the increase in the Y-axis residual stresses with velocity (Fig. 7), the time history of temperature, Y-axis plastic strain, and Y-axis stress for low and high strain rate cases (V=80mm/s, P=800W, and V=170mm/s, P=1130W) are plotted in Fig. 11. Please note that all quantities in Figs. 7 and 11 are for the top surface on the scanning path where more changes take place during forming than at the bottom surface. As seen in Fig. 11, the temperature profiles are expectedly very similar between the two cases because these cases are determined to have the same peak temperature in the first place. But the strain rate and in turn the flow stress are quite different between the two cases.

It can be seen from the time history of stress that, with the imminent arrival of the laser beam, a small tensile stress first develops due to the expansion of the preceding area, which is being heated by the laser. With the laser beam arrival and temperature rise, material tends to expand but undergoes significant compressive stress due to mechanical constraints of the surrounding material. When temperature rises further, the flow stress decreases and plastic deformation accrues, which releases the compressive stress and the absolute value of the compressive stress

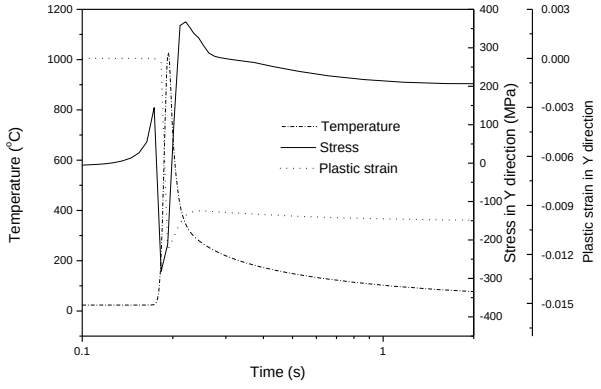


(a) V=170mm/s, P=1130W

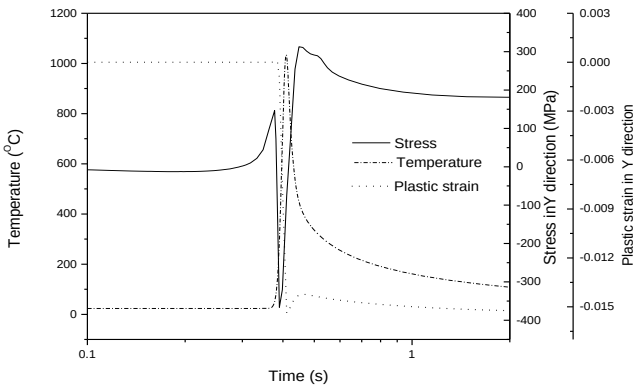


(b) V=80mm/s, P=800W

Fig. 11 Comparison of effect of high and low strain rate on residual stress

starts to reduce. After temperature reaches its maximum value, the material contracts due to the reduced temperature and the stress starts to change towards being tensile. At the same time, the tensile stress continues to rise as the material immediately ahead is being heated up by the laser beam and expands. Since the flow stress associated with the high velocity (strain rate) is higher, the tensile stress due to the thermal expansion of the material immediately ahead also rises higher. As a result, the residual stress corresponding to the high velocity remains higher than that for the low velocity, although in both cases the stress falls slightly because of the contraction of the material immediately ahead. The effect of strain rate on residual stress, however, is relatively moderate. As seen from Figs. 7 and 10, when the strain rate is nearly doubled between the lower and higher speed cases, the residual stress increases by about 15%.

## 5.4 Hardness and microstructure change

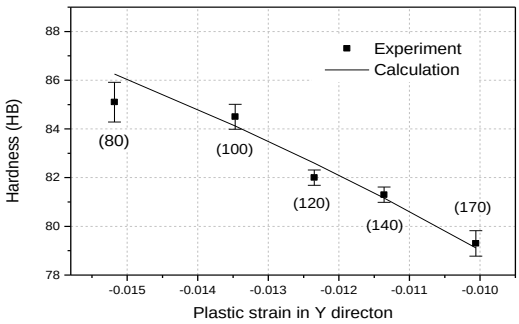


Fig. 12 Hardness vs. simulated plastic strain in Y direction under the condition of constant peak temperature (Data in brackets are the corresponding scanning velocities in mm/s)

The hardness of the deformed workpiece is measured at the top surface along the scanning path (Fig. 12). The measurement is taken 6 days after the forming is done. As seen, the hardness decreases with the increase of velocity (shown in brackets), because of the effect of work hardening. At lower velocities, the strain rate and thus flow stress is lower, resulting higher plastic strain. The higher plastic strain leads to more significant work hardening. A simple Calculated relationship between the hardness and plastic strain is also superposed on Fig.12 that agrees with the measurement data. The calculation is based on the well known empirical relationship between stress and hardness as well as $\sigma = K' \varepsilon^n$, where $\varepsilon$ is the simulated plastic strain, $n$ the work- hardening exponent for low carbon steel, and $K'$ constant. A reasonable agreement is seen.

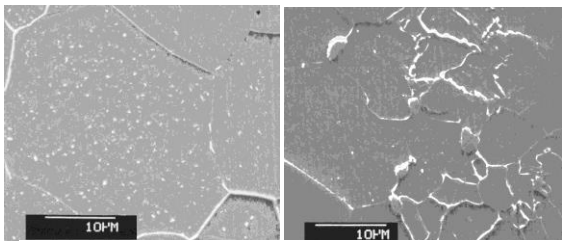


(a) (b)

Fig. 13 SEM micrograghs of the microstructures of as received (a) and scanned (b) samples near top surface (V=138mm/s, P=1380W, AISI1010)

The microstructure of the deformed workpiece is examined using scanning electron microscopy. Shown in Fig. 13 is a typical set of SEM micrograghs for the cross section of the scanning path under the condition of V=138 mm/s and P=1380 W. The simulated temperature at the top and bottom surfaces along this scanning path is about 1380 $^{o}$C and 420 $^{o}$C, respectively, as shown in Fig. 3. Shown in Fig. 13a is the microstructure of the workpiece material, low carbon steel AISI 1010, as received. Large grains of dark ferrite scattered with light-colored carbide particle are seen. Fig. 13b shows an area very close to the top surface where grain recrystallization is evident after laser forming. As mentioned earlier, the top surface undergoes significant plastic deformation at temperature above the recrystallization temperature. Laser forming may impart some beneficial properties to the workpiece top surface

under the condition. Some dissolution of carbides is also seen due to the high temperature. For the microstructure near the bottom surface, little change is observed because the region near the bottom surface undergoes much less plastic deformation (Fig. 9) and the peak temperature reached there is also much lower.

## 6. Conclusions

Laser forming simulation and experiments are conducted under that condition of constant peak temperature, which largely isolates the effects of strain rate from that of temperature. Strain rate in the laser forming process may not be extremely high but the temperature involved is high. That makes the strain rate effects on flow stress and thus deformation more significant. With strain rate increase, the thermal-induced distortion decreases and bend angle reduces. The bend angle decreases by about 30% for nearly doubled strain rate under the conditions used. Residual stress in the Y direction increases moderately with strain rate. For the doubled strain rate, residual stress increases by about 15% under the conditions used. With the strain rate increase, the hardness of the formed sample decreases due to the reduced work hardening. Recrystallization and dissolution of hard particles occur near the top surface of the workpiece material used where temperature is higher and plastic deformation is more severe.

## References


[1] Magee, J., Watkins, K. G., Steen, W. M., "Advances in laser forming," Journal of Laser Application, Vol. 10, 1998, pp. 235-246.

[2] Vollertsen, F., "Mechanism and models for laser forming," Laser Assisted Net Shape Engineering, Proceedings of the LANE'94, Vol. 1, 1994, pp. 345-360.

[3] Arnet, H., and Vollertsen, F., "Extending laser bending for the generation of convex shapes," IMechE Part B: Journal of Engineering Manufacture, Vol. 209, 1995, pp. 433-442.

[4] Vollertsen, F., Geiger, M., and Li, W. M., "FDM and FEM simulation of laser forming a comparative study," Advanced Technology of Plasticity, Vol. 3, 1993, pp. 1793-1798.

[5] Hsiao, Y.-C., Shimizu, H., Firth, L., Maher, W., and Masubuchi, K., "Finite element modeling of laser forming," Proc. ICALEO '97, Section A, 1997, pp. 31-40.

[6] Alberti, N., Fratini, L., and Micari, F., "Numerical simulation of the laser bending process by a coupled thermal mechanical analysis," Laser Assisted Net Shape Engineering, Proceedings of the LANE'94, Vol. 1, 1994, pp. 327-336.

[7] Magee, J., Watkins, K. G., Steen, W. M., "Edge effects in laser forming," Laser Assisted Net Shape Engineering 2, Proceedings of the LANE'97, Meisenbach Bamberg, 1997, pp. 399-406.

[8] Bao, J. and Yao, Y. L., "Analysis and prediction of edge effects in laser bending," to be presented ICALEO'99, San Diego, CA, Nov. 1999.

[9] Li, W., and Yao, Y. L., "Laser forming with constant line energy," submitted to International Journal of Advanced Manufacturing Technology, 1999.

[10] Boley, B., and Weiner, J. H., Theory of Thermal Stresses," Dover Publications, In, 1997.


## Meet the Authors


Wenchuan Li is currently a Ph.D. candidate and Y. Lawrence Yao an Associate Professor in the Department of Mechanical Engineering at Columbia University, where Yao also directs the Manufacturing Engineering Program. Yao has a Ph.D. from Univ. of Wisconsin-Madison.